GOETHITE ON MARS: A LABORATORY STUDY

J. B. POLLACK, D. PITMAN, B. N. KHARE,
and C. SAGAN

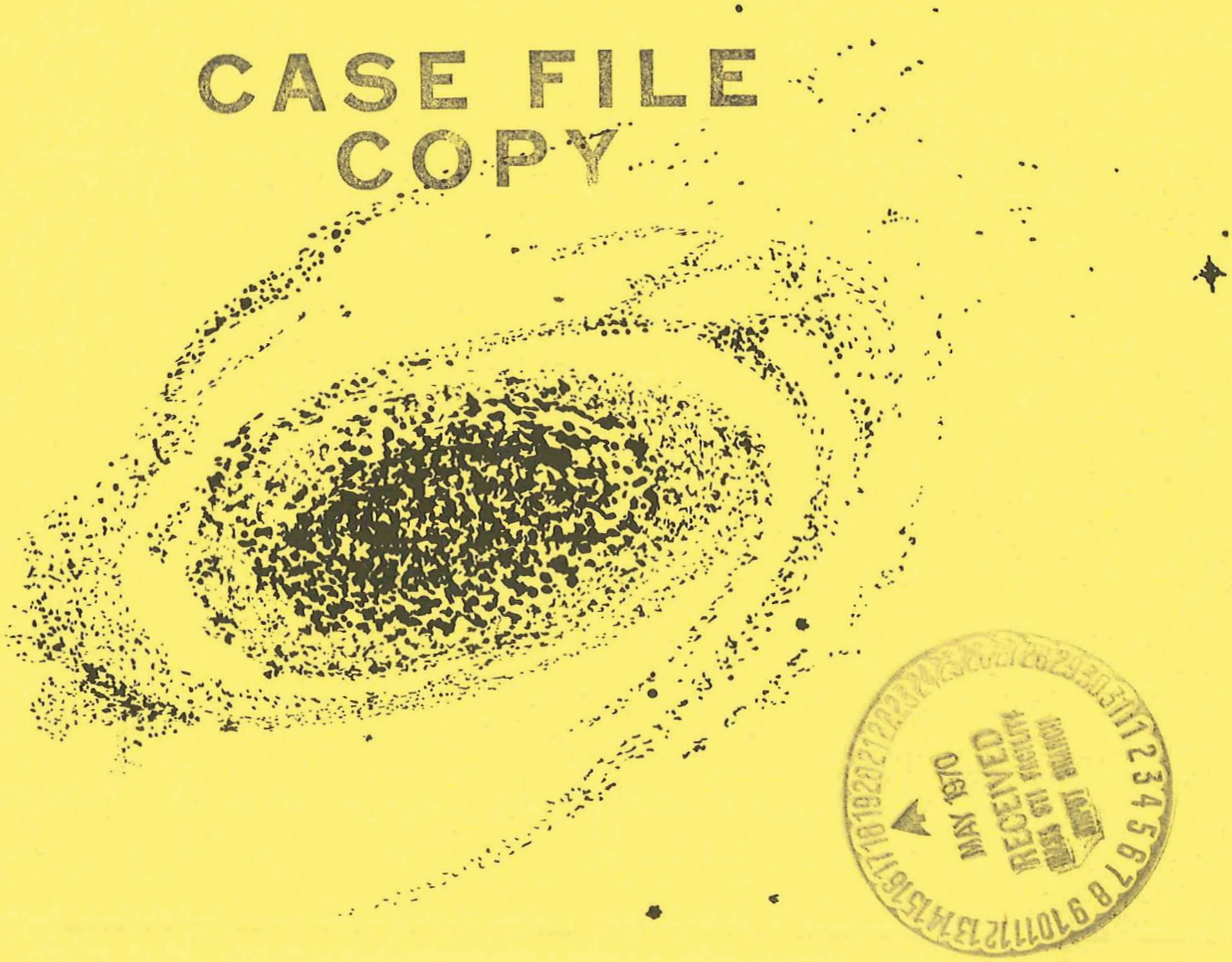

Smithsonian Astrophysical Observatory
SPECIAL REPORT 314

SAO Special Report No. 314

GOETHITE ON MARS: A LABORATORY STUDY OF PHYSICALLY AND CHEMICALLY BOUND WATER IN FERRIC OXIDES

James B. Pollack, Douglas Pitman, Bishun N. Khare, and Carl Sagan

May 15, 1970

Smithsonian Institution
Astrophysical Observatory
Cambridge, Massachusetts 02138

908-47

TABLE OF CONTENTS

LIST OF ILLUSTRATIONS

LIST OF TABLES

ABSTRACT

A thermogravimetric analysis of the decomposition of goethite-rich samples of limonite and measurement of the equilibrium vapor pressure of the water physically bound in the sample are performed. The heats of sorption for the physically bound component are determined; an activation energy of 29 ± 3 cal/mole is found between 225° and 390°C. The goethite-hematite reaction is of order 1/2, reasonable for the powders used. The results imply that physical sorption will tend to take place preferentially over condensation. This tends on Mars to inhibit the formation of a water polar cap. The atmospheric water-vapor pressure should vary with the seasons because of the temperature dependence of physical sorption. Since the amount of this variation seems to be in accord with the spectroscopic observations, an alternative exists to the hypothesis that the greater water-vapor partial pressure in the spring hemisphere indicates meridional transport of water vapor and an ice polar cap. Because of their superior topographical resolution, spacecraft correlations of temperature and water-vapor abundance seem to be the most promising tool for establishing whether sorption or condensation controls the seasonal and topographical variations in the atmospheric water-vapor content.

RÉSUMÉ

Nous avons fait une analyse thermogravimétrique de la décomposition d'échantillons de limonite riches en goéthite et une mesure de la pression de vapeur à l'équilibre de l'eau physiquement unie à l'échantillon. Nous avons déterminé les chaleurs de sorption du constituant physiquement uni; nous avons trouvé une énergie d'activation de 29 ± 3 cal/mole entre 225 et 390° C. La réaction goéthite-hématite est de l'ordre de 1/2, ce qui est raisonnable pour les poudres employées. Les résultats impliquent que la sorption physique aurait tendance à avoir lieu de préférence à la condensation. Ceci tend, sur Mars, à empêcher la formation d'une calotte polaire d'eau. La pression atmosphérique de la vapeur d'eau devrait varier avec les saisons car la sorption physique dépend de la température. La valeur de cette variation semble être en accord avec les observations spectroscopiques, il existe donc une autre solution à l'hypothèse qu'une plus grande pression partielle de la vapeur d'eau dans l'hémisphère au printemps indiquerait un transport méridional de la vapeur d'eau et une calotte polaire de glace. A cause de leur meilleure résolution topographique, les corrélations entre la température et la quantité de vapeur d'eau, obtenues par vaisseaux spatiaux, semblent devoir être le meilleur moyen pour déterminer si la sorption ou la condensation sont à la base des variations saisonnières et topographiques dans la contenance de l'atmosphère en vapeur d'eau.

КОНСПЕКТ

Представляется на рассмотрение термогравиметрический анализ распада образцов лимонита, обогащенных $HFeO_2$ и измерения равновесного парового давления воды, присутствующей в образце. Была определена теплота сорпции присутствующей компоненты; энергия активации, в 29 ± 3 кал/моль, была найдена между $225^{\circ}C$ и $390^{\circ}C$. Реакция $HFeO_2$ с окисью железа является порядка 1/2, что приемлимо для используемых порошков. Полученные результаты означают, что физическая сорпция имеет место преимущественно во время конденсации, что способствует задержанию формирования водяной полярной шапки на Марсе. В результате зависимости физической сорпции от температуры, атмосферное давление вода-пар должно меняться со сменой времен года. Так как величина этих измерений согласуется со спектроскопическими наблюдениями, то представляется возможным следующее предположение: увеличение частного давления вода-пар в теплом полушарии указывает на меридиональное перемещение водяных паров и ледяной полярной шапки. Благодаря превосходному топографическому анализу, температурные корреляции, полученные во время космических полетов, и избыточное давление вода-пар являются наиболее обещающими факторами в разрешении вопроса, зависит ли сезонное и топографическое изменение содержания воды-пара в атмосфере от сорпции или от конденсации.

GOETHITE ON MARS: A LABORATORY STUDY OF PHYSICALLY AND CHEMICALLY BOUND WATER IN FERRIC OXIDES

James B. Pollack, Douglas Pitman, Bishun N. Khare, and Carl Sagan

1. INTRODUCTION

Dollfus (1957), Sharonov (1961), Sagan, Phaneuf, and Ihnat (1965), Binder and Cruikshank (1963), and Pollack and Sagan (1967) have discussed the possible presence of limonite on Mars. Limonite is a common terrestrial rock containing the hydrated ferric oxide mineral, goethite. To understand better the behavior of goethite on Mars, we have undertaken a series of laboratory measurments of its water components. Goethite contains both a physically bound component, which is present as water of sorption, and a chemically bound component, which has been incorporated into the crystal structure. Unlike the physically bound component, the chemically bound water is not present as identifiable water molecules. Its atoms have been rearranged with those of ferric oxide, in the proportion 1:1, to form a structure with individual hydrogen atoms each situated symmetrically between a pair of oxygen atoms (Goldsztaub, 1935). When heated to high temperatures, goethite is transformed into its anhydrous derivative, hematite, which has a different crystal structure, and water vapor is released.

Below we describe a thermogravimetric analysis of the decomposition of goethite and measurements of the equilibrium vapor pressure of the physically bound component. From the data, we obtain heats of sorption for the physically bound component and an activation energy and order of the reaction involving the release of the other water component. Finally, we consider the application of the results to Mars.

This work was supported in part by grants NGR 09-015-023 and NGR 33-010-082 from the National Aeronautics and Space Administration.

2. DESCRIPTION OF THE SAMPLES

We investigated the properties of two naturally occurring limonite samples obtained from Ward's Natural Science Establishment, Rochester, New York. One is indigenous to Cartersville, Georgia; the other, to Biwabik, Minnesota. These samples have been studied thermogravimetrically and spectrophotometrically by Sagan et al. (1965). The two minerals are texturally quite distinct but, as we see below, are chemically similar. The Georgia sample occurs naturally as a fine yellow powder with an average dimension of 70 μ, while the Minnesota sample is in an unpulverized state. This second sample was ground and passed through a screen with 44-μ mesh openings. The presence of goethite in each sample was verified by a Debye-Scherer X-ray diffraction analysis, which also indicated the presence of significant amounts of quartz.

Determinations of the weight fraction of iron and hydrogen present in the samples were made by the Skinner and Sherman Laboratories of Newton, Massachusetts. They employed the phenanthroline method to determine the total iron content (American Public Health Association, 1965) and found the hydrogen content by heating the specimens to 1000°C in a homemade vacuum-fusion analyzer. Assuming that all the iron is present as Fe_2O_3 and all the hydrogen as H_2O, we derive the mass fractions shown in columns A and B of Table 1. The water-vapor abundance so determined is the sum of the chemically and physically bound components. Requiring a 1:1 ratio by number between chemically bound water and ferric oxide, we separate the two components, with results shown in columns C and E of Table 1.

As a check on the above procedure, we performed a thermogravimetric analysis of the Cartersville specimen. The sample was heated at a fixed temperature for 8-hr periods until the weight of the solid component became constant; then the sequence was repeated at higher temperatures. Dry nitrogen flushed the tube furnace during heating. The results are shown in Figure 1.

The slow, continuous variation of the mass-loss curve is attributed to a loss of the physically bound water, while the almost discontinuous change near 200°C represents a decomposition of goethite into hematite with the release of the chemically bound component (Posnjak and Merwin, 1919). Figure 1 suggests that a total weight loss of 7.5% had been sustained when the temperature reached 400°C, in good agreement with the total water content of 8.3% inferred from the chemical analysis of the H_2 content at 1000°C. From the magnitude of the near discontinuity, we infer a weight percentage of 6.4% for the chemically bound component, which is in agreement with the figure inferred from the iron and hydrogen analyses. We conclude that the amounts of goethite and water derived should be quite close to the true values. Below we use Figure 1 in studying the kinetics of the decomposition of goethite.

Table 1. Percentage by weight of the Fe_2O_3 and H_2O content of the samples.*

	Fe_2O_3	Total H_2O		Chemically bound H_2O		Physically bound H_2O	
Sample	A	B	C	D	E	F	G
Cartersville, Georgia	57.2%	8.3%	7.75%	6.4%	6.4%	1.9%	1.11%
Biwabik, Minnesota	72.6%	9.7%	—	8.2%	—	1.5%	—

*The results in columns A, B, D, and F were obtained from the phenanthroline and vacuum-fusion analyses, while the remaining columns were inferred thermogravimetrically.

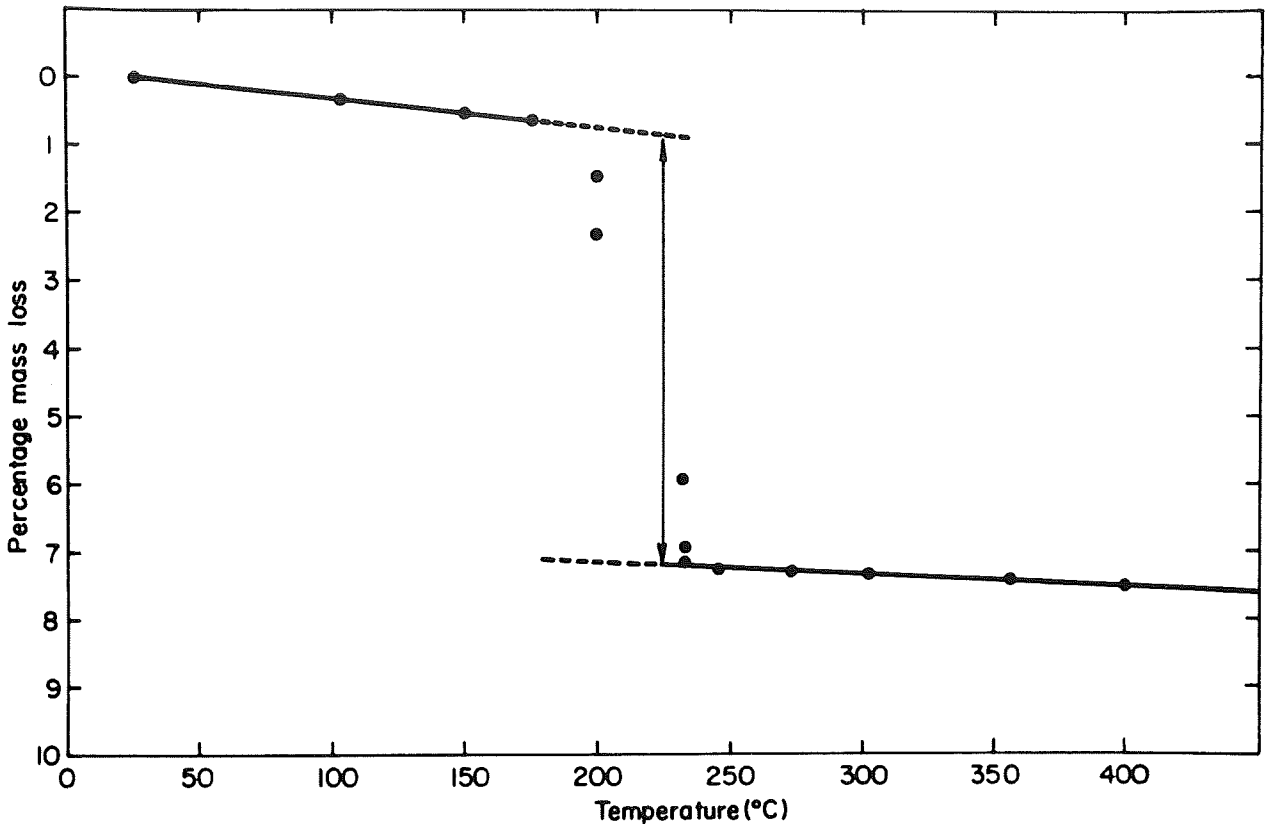

Figure 1. A thermogravimetric analysis of the Cartersville, Georgia, sample. It was heated to progressively higher temperatures, with the percent mass loss (with respect to the initial value) measured at the end of each heating cycle. The sudden loss of water near 200 °C reflects an outgassing of the chemically bound component and subsequent conversion of the sample to hematite, while the more gradual outgassing is attributable to the physically bound water component.

3. VAPOR-PRESSURE MEASUREMENTS OF THE PHYSICALLY BOUND COMPONENT

We measured the equilibrium vapor pressure of water over both samples between -50° and +150°C. Measurements in this temperature domain refer to the physically bound component (cf. Figure 1). It is extremely difficult to obtain directly the corresponding information for the chemically bound water: at temperatures above 130°C the equilibrium vapor pressure over these minerals is greater than it is over liquid water (Pollack, Wilson, and Goles, 1969; henceforth referred to as Paper I). Accordingly, condensation will occur at such temperatures before equilibrium is attained. On the other hand, at temperatures below 130°C the time to reach equilibrium is at best on the order of a year (Paper I), and so formidable experimental difficulties present themselves.

The apparatus in which the measurements were performed is represented schematically in Figure 2 and photographically in Figure 3. A ferric oxide mineral sample was vacuum sealed into the system and brought to liquid-nitrogen temperatures, and the entire system evacuated by a mechanical pump and Hg-diffusion pump operating in tandem. By pumping for about a day, we obtained pressures $\sim 10^{-4}$ torr (1 torr = 1 mm Hg). The sample was then isolated from the vacuum pump and placed in a constant-temperature bath at the temperatures of interest. Constant-temperature baths of carbon tetrachloride, carbon disulfide, water ice, chlorobenzene, and mixtures of dry ice and acetone were used to attain temperatures below room temperature, while a resistance furnace was employed for the higher temperatures. The temperature of the sample was monitored by a thermocouple buried within it.

After the sample had reached the temperature of the bath, its portion of the system was connected to a pressure sensor. For pressures above 10 torr a mercury manometer was employed; at lower pressures a "Barotron" capacitance pressure gauge, linked to a strip-chart recorder, was used. In all cases, after a sufficient period of time, a constant-pressure reading

was obtained, indicating that equilibrium had been established. We estimate the time needed to approach equilibrium from initial vacuum conditions to be on the order of a few hours.

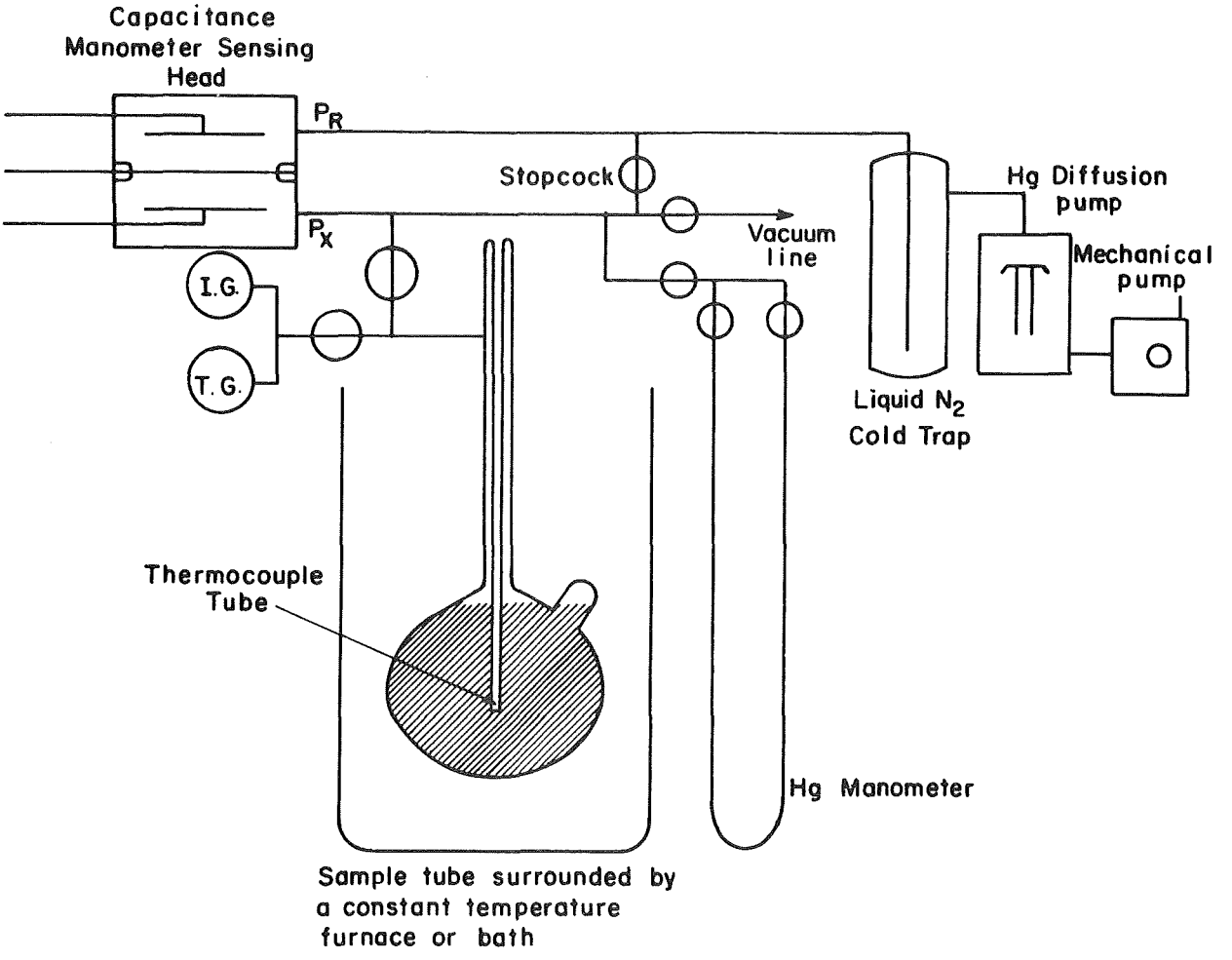

Figure 2. Schematic diagram of the apparatus used to measure the equilibrium vapor pressure of the limonite samples. The sample is introduced into the flask, and its temperature is controlled by the constant-temperature furnace (for high temperatures) or bath (for low temperatures). The diffusion and mechanical pumps are used to establish vacuum conditions, and their performance is monitored by the subsystems labeled I. G. (ionization gauge) and T. G. (thermocouple gauge). The temperature of the sample is measured by a thermocouple inserted into it (which is not related to T. G.), and its vapor pressure is measured at high pressures by the Hg manometer and at low pressures by the capacitance manometer. The P_X and P_R portions of the capacitance manometer are connected to the unknown (i. e. , sample) pressure line and to a reference pressure line (at vacuum conditions), respectively. The volume between the top of the sample and the capacitance manometer was 39 cc. The Biwabik and Cartersville samples occupied volumes of 60 and 42 cc and had masses of 59 and 82 g, respectively.

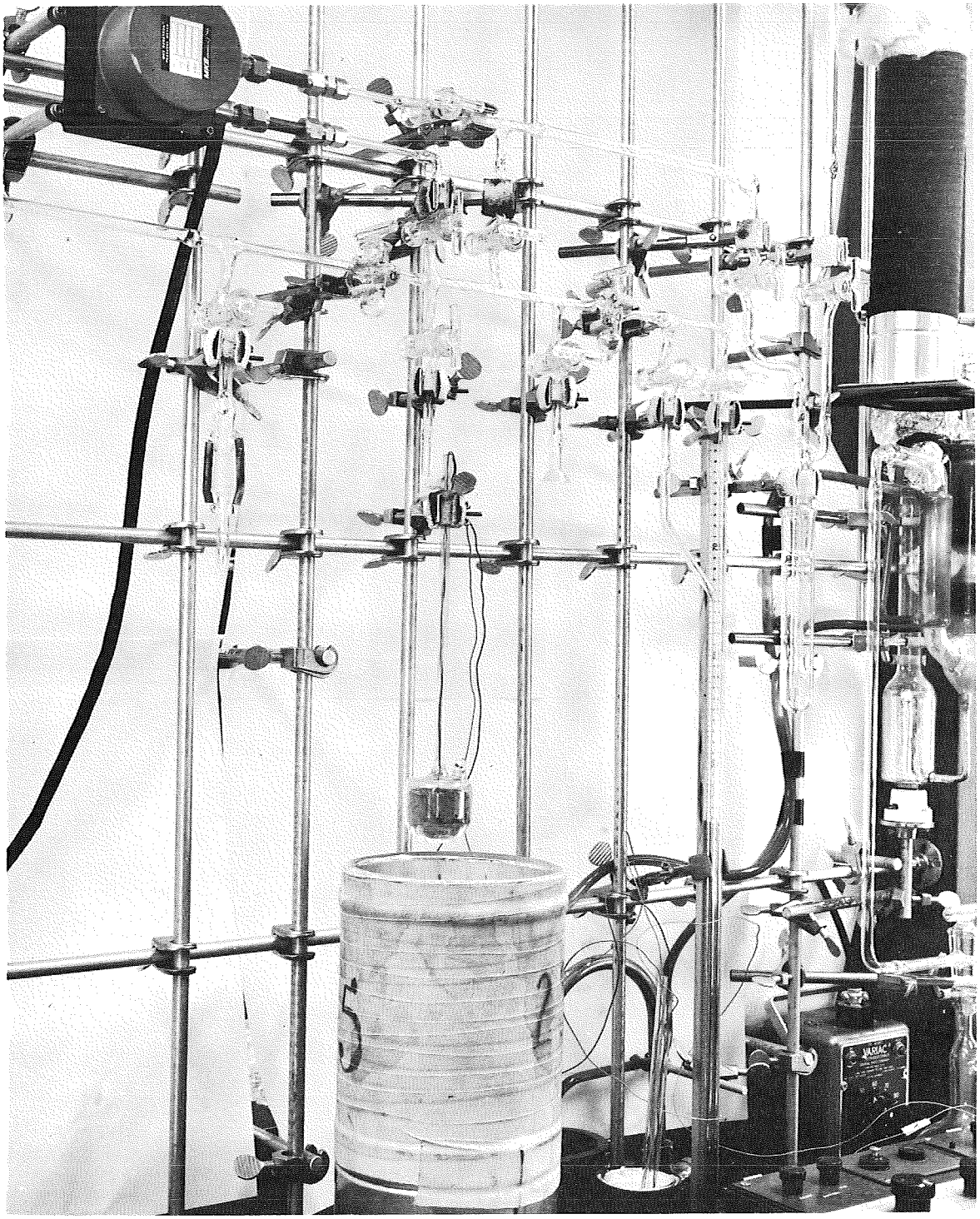

Figure 3. Photograph of the actual apparatus. Compare with the schematic diagram given in Figure 2.

Figures 4 and 5 summarize the results. Curve 1 represents the equilibrium vapor pressure above liquid and solid water for temperatures above and below 0°C, respectively, while the other curves indicate our results for the ferric oxide minerals. The initial set of measurements at one sequence of temperatures is given by curve 2. Subsequently, we diminished the amount of physically bound water present in the sample and then remeasured the vapor pressure, with the results shown in curve 3. In a similar fashion curves 4 and 5 were obtained. To decrease the amount of sorbate, we either expanded the gas into a larger volume or, more typically, connected the sample to the liquid-nitrogen cold trap and vacuum pumps and evacuated the system for at least a few hours. The last pumping operation for each sample, which took place between curves 4 and 5, occurred over an interval of several days with the sample at a temperature of 150°C. We found that it became progressively more difficult to displace the curves from the previous values. On several curves, after measuring the pressures at the peak temperature point, we lowered the temperature and performed further pressure measurements. The results for this last set of data coincided with the curve determined from the initial set of observations. This finding confirms that the measurements refer to equilibrium pressures.

Two tests were made to ensure that the observed vapor was almost entirely water vapor. First, for curve 2 of the Cartersville sample, the temperature was raised sufficiently so that the vapor pressure exceeded 26 torr. As the manometer was at room temperature, condensation of liquid water should have occurred when the total pressure approached 26 torr, provided the gas was almost entirely water vapor. As can be seen from the measured points of Figure 4, a break in the measured curves does occur at 26 torr. In addition, a more detailed analysis was made of the vapor for several measurements of the Biwabik sample. Equilibrium was allowed to occur throughout the system. Then the vapor in a portion of the system containing the pressure gauge was isolated from the sample, and a cold finger in this section was placed in liquid nitrogen. The pressure was found to decrease to a few percent of its initial value, reflecting the presence of noncondensable components in the vapor. A mass-spectrometric analysis of the remaining fraction of the vapor

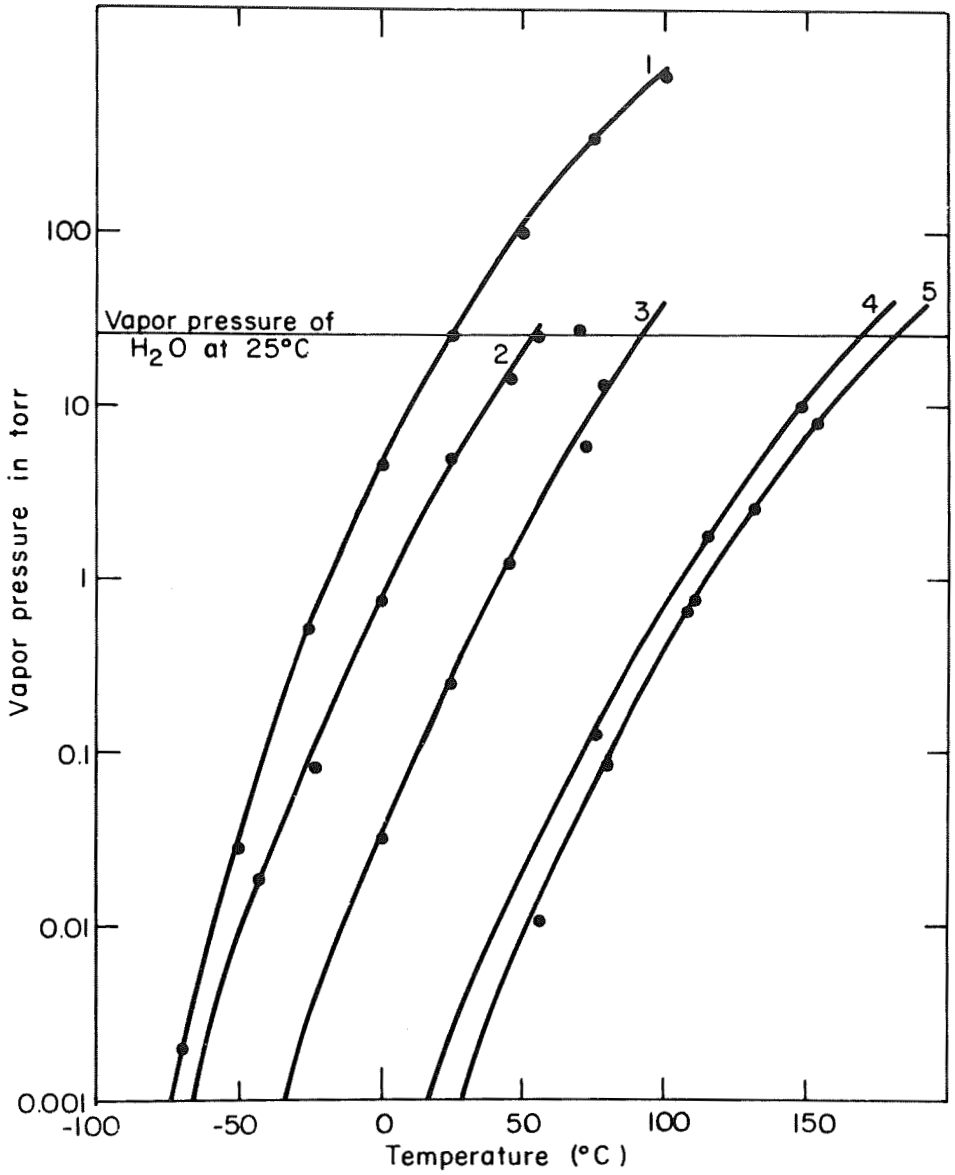

Figure 4. Points along cuves 2, 3, 4, and 5 represent the measured vapor-pressure values for the Cartersville, Georgia, sample. Curve 2 was first measured, and subsequently the system was vacuum pumped for a number of hours. The resulting vapor-pressure curve is given by curve 3, reflecting a decrease in the sorbate volume. In a similar fashion, curves 4 and 5 were obtained. Curve 1 is the equilibrium vapor-pressure curve of liquid water and ice, at temperatures above and below 0 °C, respectively. Curve 1 was measured with our apparatus and is in excellent agreement with standard, tabulated values.

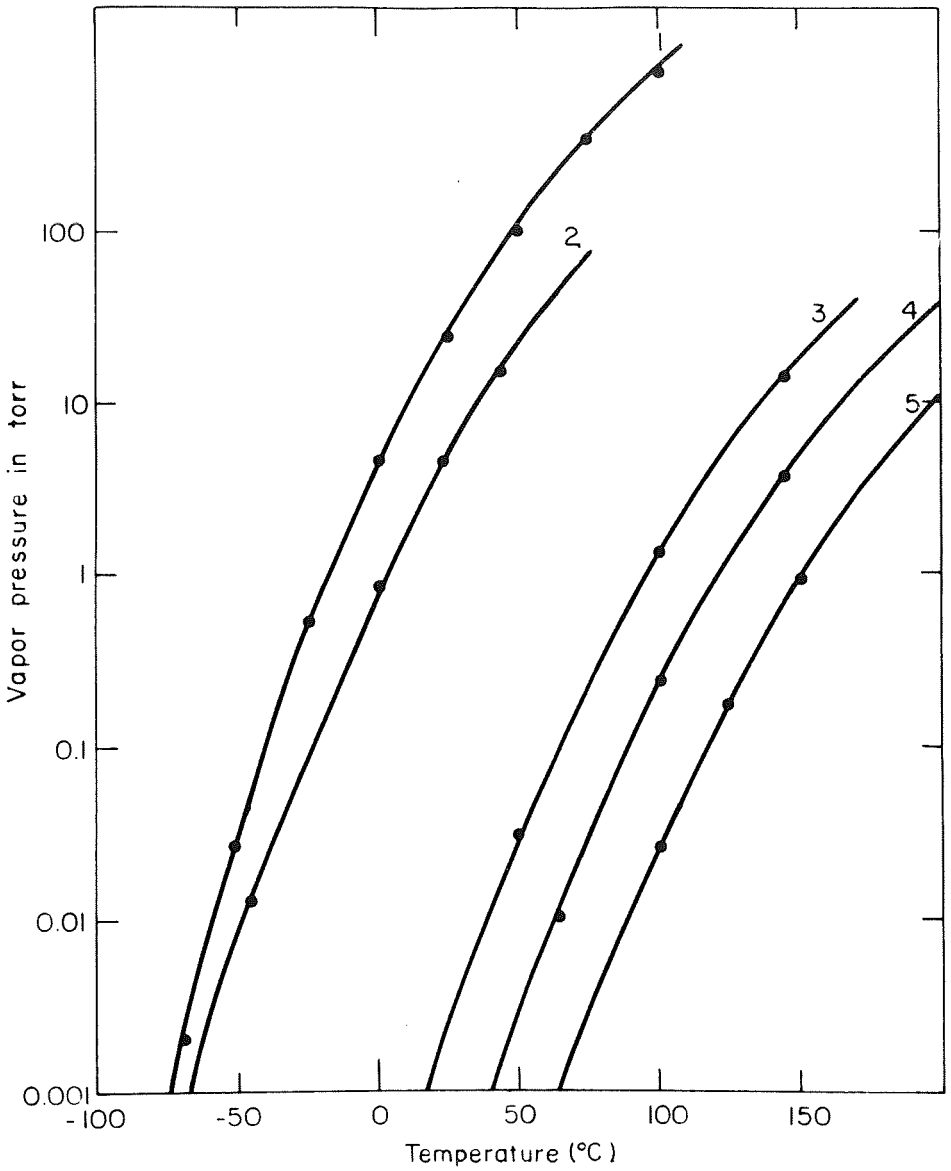

Figure 5. Vapor-pressure curves for the Biwabik, Minnesota, sample. The curves have a similar meaning to those in Figure 4.

indicated the presence of a small amount of gas with a mass number 16, possibly methane, the presence of which deserves further study. Finally, an ice-water bath at 0 °C replaced the liquid nitrogen at the cold trap. The resulting pressure was almost identical with the equilibrium vapor of water over ice at 0 °C. Thus, except for a few percent of other gases, the observed vapor consisted of water.

The curves obtained for the two samples are very similar. This finding indicates that changes in the proportion of minor mineral constituents, including quartz, do not drastically alter our results.

Above, we found that the equilibrium vapor pressure of the physically bound water component is a function not only of the temperature of the limonite sample but also of the sorbate volume, i. e., the amount of physically bound water present. For this reason, we obtained a series of curves, rather than a unique curve as there would be for the chemically bound component. Such a result is typical of the behavior of all gases that experience sorption by solid materials (Dushman, 1962) and is analogous to the behavior of gases dissolved in liquids.

4. THERMODYNAMIC CALCULATIONS

Using the data presented above, we derive several thermodynamic variables of interest. We begin by estimating the heat of sorption, i.e., the heat required to cause a mole of physically bound water to undergo a phase change to the vapor state. In Figures 6 and 7, the curves of Figures 4 and 5 have been replotted on a graph whose coordinates are log pressure and reciprocal temperature. The slopes of the curves on these new graphs can be directly related to the heat of sorption through the Clausius-Clapyeron equation. We see that to first order the points for a given curve lie along a straight line, indicating that the heat of sorption does not vary rapidly with temperature.

Table 2 summarizes the heats of sorption Q derived from each of the curves. Also given is the observed or extrapolated pressure P_{75} at 75°C, so as to define more quantitatively the differences between the various curves. For both samples there is a systematic increase in Q with a decrease in the partial pressure, or equivalently of the amount of sorbate at a given temperature. We also see that the values of Q for the two samples at similar values of P_{75} are in good agreement. An estimated uncertainty in the value of Q of about ± 0.5 kcal/mole is implied by the scatter of the data points and by comparison of the results for the two samples.

In order for physical sorption to occur instead of condensation, the change in free energy for the first process should be greater than that for the second. While we cannot exactly equate latent heats with changes in free energy, we can generally expect that the heat of sorption should be comparable to or greater than the latent heat of condensation in order that sorption take place. Comparing the heats given in Table 2 with the values of 10.8 and 12.2 kcal/mole for the latent heats of liquid water and ice, respectively, we see that this condition is met.

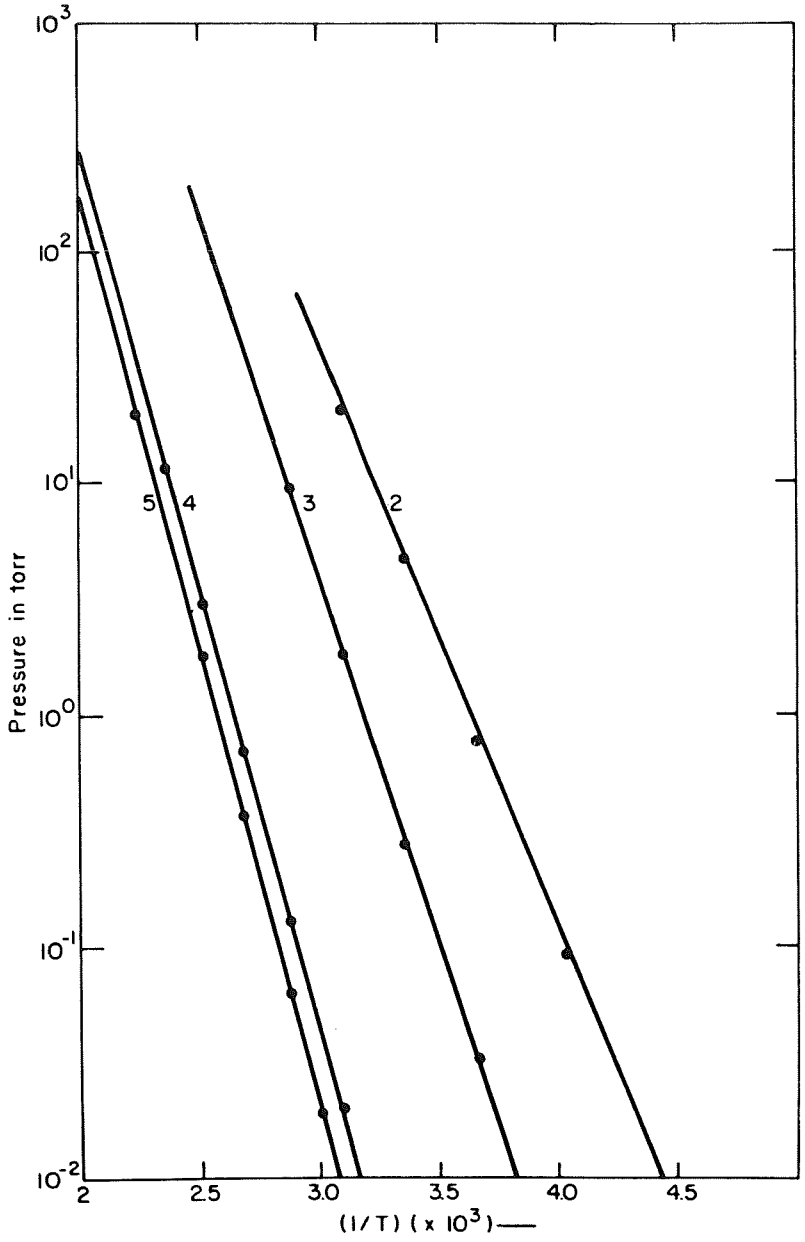

Figure 6. A replotting of Figure 4 with the horizontal coordinates in units of $1/T \times 10^3/°K$. The slope of each curve is proportional to the heat of sorption.

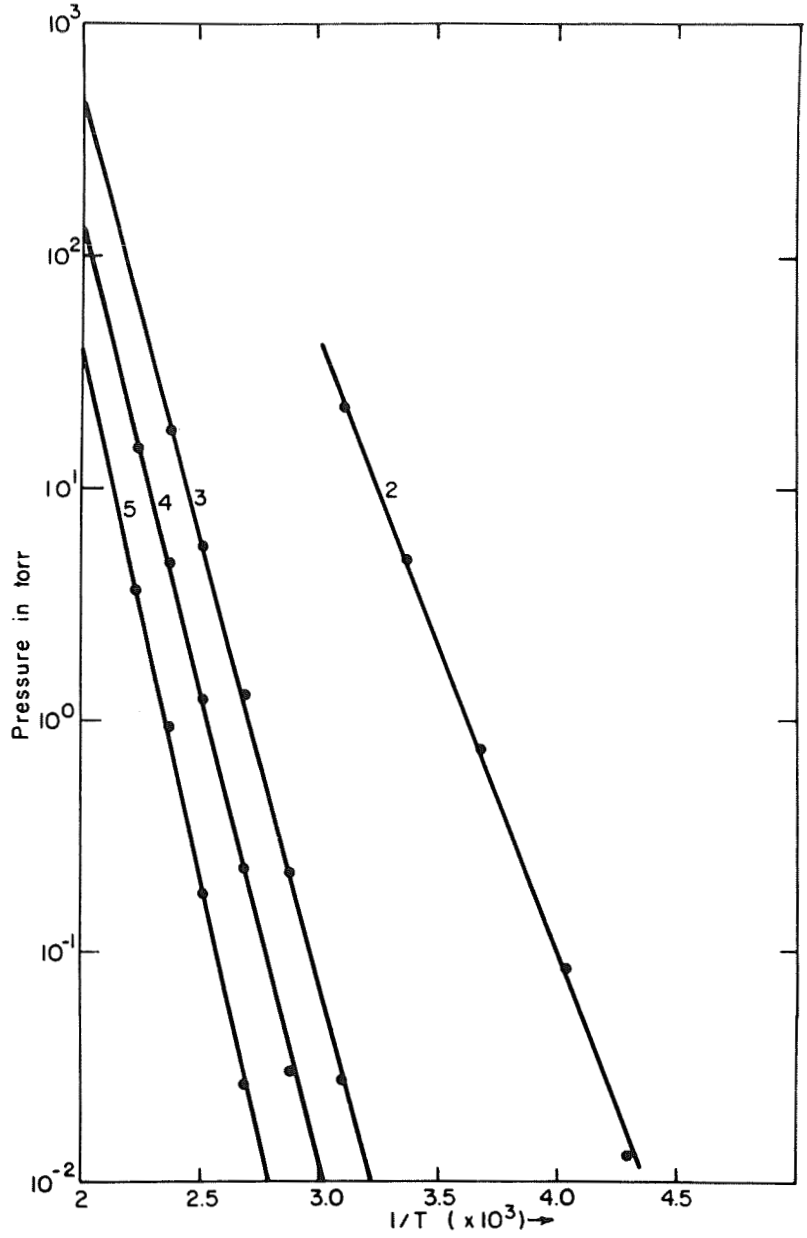

Figure 7. A replotting of Figure 5. See the description of Figure 6.

Table 2. Heats of sorption Q and equilibrium vapor pressures of water P for pulverized limonite.

	Biwabik Sample		Cartersville Sample	
Curve	Q (kcal/mole)	P (at 75 °C) (torr)	Q (kcal/mole)	P (at 75 °C) (torr)
2	12.1	7.1×10	11.8	7.2×10^{1}
3	17.5	2.2×10^{-1}	14.2	9.5×10^{0}
4	18.5	2.95×10^{-2}	17.5	1.35×10^{-1}
5	20.9	2.95×10^{-3}	18.0	6.3×10^{-2}

The deduced increase of the heat of sorption with decreasing sorbate volume is in accord with the behavior of many similar systems (Dushman, 1962). Such a phenomenon can be understood in terms of the molecular environment of a molecule that can readily escape. When the sorbate volume is large, there may be a number of other water molecules in its immediate environment, and so the molecular forces will be quite similar to those near a molecule in the top layer of the condensate. Accordingly, we would expect the heat of sorption to be quite similar to the latent heat for condensation, in agreement with the results of Table 2. When the sorbate volume is small, a molecule capable of escaping will experience forces principally from the atoms of the host mineral, and in accord with the discussion of the previous paragraph, this will generally result in heats of sorption larger than the value for the latent heat of condensation.

The physically bound water may be attached to the limonite in three possible ways. It may be adsorbed to the surface of the sorbent, absorbed in the interior, or condensed as capillary water. Unfortunately, the present data do not allow us to distinguish among these possibilities. However, since the number of molecules of physically bound water can be of the same order as the number of sorbent molecules, absorption may be the dominant mode (cf. Table 1).

Measurements of the specific heat of goethite provide a way of determining its thermodynamic properties at temperatures directly relevant for terrestrial and Martian conditions. Unfortunately, these results may be seriously influenced by the presence of the physically bound component, especially if a powder is used in the study. Some physically bound water will be released as the specimen is heated. The specific heat of many minerals is about 0.25 cal/g (K°). Such a figure for goethite implies a molar specific heat of 44 cal/mole (K°) or 4.4 kcal/mole (100 K°). Since the heat of sorption is typically 15 kcal/mole and since limonite powders generally contain a sorbate molar fraction on the order of unity (cf. Table 1), the measured specific heats may be significantly influenced by this component. Perhaps the use of solid specimens of goethite will help reduce this problem.

We next consider the decompostion of goethite into hematite, with an accompanying release of the chemically bound water. We first discuss the order n of this reaction defined by

$$\frac{dw}{dt} = - kw^n \quad , \tag{1}$$

where w is the fraction of goethite remaining at time t normalized so that w (t = 0) = 1. The parameter k is the rate constant. Lima de Faria (1963) has measured the percent mass loss of goethite during decomposition, proportional to (1 - w), as a function of time at a variety of fixed temperatures. His curves show a significant curvature at high mass loss, indicating $n > 0$. On the other hand, they approach their asymptotic value more rapidly than does the theoretical curve for $n = 1$. A quantitative comparison of equation (1) with these data indicates $n \simeq 1/2$.

It may at first appear odd that there should be any dependence of the rate on w. In understanding the above result, we should take into consideration that the sample was a powder. We postulate that the goethite-hematite phase boundary is initially defined by the surface area and advances into the grain with time. Suppose that the rate of dehydration is proportional to the

instantaneous area of the phase boundary. Then dw/dt will vary as $w^{2/3}$ for spheres, as $w^{1/3}$ for long cylinders, and as w^{0} for flat, thin plates. Since a powder is a mixture of such shapes, it seems reasonable that, approximately, $dw/dt \propto w^{1/2}$, as observed. Alternatively, decomposition may occur at the same rate at the phase boundary, but the diffusion of water vapor from the phase boundary to the surface may take longer the deeper the boundary is.

A quantity of great interest is the activation energy E_a of the chemically bound component, which defines the temperature dependence of the rate constant through the Arrhenius relation

$$k = C\, e^{-E_a/RT}, \qquad (2)$$

where R is the universal gas constant, T the absolute temperature, and C a proportionality constant. In practice, E_a may itself be a function of T. We now describe three independent estimates of E_a. Lima de Faria estimated E_a to be 19.8 kcal/mole from his dehydration curves at 350°, 400°, and 450°C. We believe there is an error in this result. His curves at 300°, 325°, and 350°C, all of which are well defined, show an appreciable linear portion. An extrapolation of the linear portion of the curve to zero mass loss implies a nonzero and a positive value for the time coordinate; i.e., there is initially less mass loss than expected from the extrapolation. We interpret this as an indication of the finite time required for the interior of the sample to reach the temperature of the furnace. In the above discussion of the order of the reaction, the zero point of the time scale was appropriately shifted. Lima de Faria's curves at 400° and 450°C are defined by relatively few points and lie mostly within the time zone where the other curves show an appreciable lag in outgassing. Accordingly, we consider the value of 19.8 kcal/mole inferred for E_a as only a lower limit to its true value. Using the well-defined slopes for the curves at 350°, 325°, and 300°C, we derive a value for E_a of 33.5 ± 5 kcal/mole, where the error includes the uncertainty in the zero point of the time scale. The error estimate is probably a conservative one since the value of E_a found from the slopes at 325° and 350°C agrees to better than 1 kcal/mole with that obtained from the 300° - 325°C pair.

A second estimate of E_a can be obtained by combining the dehydration curve shown in Figure 1 with an analogous curve obtained for the same sample at significantly higher temperatures by Sagan et al. (1965). From the time scales assigned to the points in Figure 1, we estimate that a sample of goethite held at a temperature of 225 ± 5°C will dehydrate to e^{-1} of its original weight in 67 hr. Sample solutions of the one-dimensional heat-conduction equation indicate that temperature phase lags through the powder are negligible for these measurements. In the earlier measurements of Sagan et al., the temperature of the sample was increased at a rate of 20 C°/min and the mass loss measured. Thermocouple measurements indicated a temperature phase lag in the interior of samples of no more than 0.5°K (J. P. Phaneuf, 1968, private communication), negligible for our considerations. A straightforward integration of equations (1) and (2) for dT/dt constant yields the following relationship between w and T:

$$F_n(w_f, w_i) = \frac{CRT_f^2}{E_a(dT/dt)} \left[1 - \frac{2}{E_a/RT_f} + \frac{6}{(E_a/RT_f)^2} \right] \exp\left(-\frac{E_a}{RT_f}\right) . \quad (3)$$

The subscripts i and f indicate, respectively, initial and final values; $F(w_f, w_i)$ is given by

$$F_n = \begin{cases} \ell n\,(w_f/w_i) , & n = 1 \\ (1 - n)\left[w_f^{(1-n)} - w_i^{(1-n)} \right] , & n \neq 1 \end{cases} . \quad (4)$$

In deriving equation (3), we have used an expansion of the exponential integral of second order for large values of the argument (Chandrasekhar, 1960). The data of Sagan et al. imply $w_f = 1/2$ at $T_f = 390 \pm 10$°C.

Combining these two sets of thermogravimetric measurements, we can obtain a value for E_a from equation (3). The value of C is found from using the lower temperature data in equation (2) and the integral form of equation (1). We find E_a to be 29 ± 2.5 kcal/mole between 225° and 390°C; E_a has only a very slight dependence on n for n between 0 and 1. The sample used by Lima de Faria was quite pure, while ours contained only about 50% goethite. Thus, it is interesting that the two values of E_a obtained should be very similar, indicating no strong dependence upon the presence of other materials.

A final estimate of E_a can be obtained by combining the measurements of Figure 1 at 200° and 233°C. After 18.5 hr of heating at 200°C, a fractional mass loss of 0.82% was recorded, while after an additional 65.7 hr, a mass change of 0.85% was found. Although part of the first session's loss could be physically bound water, an examination of Figure 1 implies that this additional source of vapor is probably not enough to account for the near equality in the fractional losses despite a factor of 3 difference in heating times. These measurements occur near w = 1, where the mass loss should vary approximately linearly with time. Thus, there appears to be something wrong with the measurements at 200°C. Successive measurements at 233°C of 67, 119.1, and 143.8 hr gave losses of 3.67%, 1.02%, and 0.15%, respectively. At the end of the last measurement, the goethite had been almost completely converted to hematite, and indeed color changes were apparent even after the first measurement at 200°C. The integral form of equation (1) with n = 1/2 and equation (2) can be employed to find an activation energy from the above data. If we use the second measurement at 200°C and the first one at 233°C, we find a value for E_a of 25.1 kcal/mole, in possible agreement with our estimates above, whereas the average value of the results at 200°C and the first measurement at 233°C leads to a value of 18.3 kcal/mole, in disagreement with our estimates. It is difficult to see how the last value for E_a can be raised to the previous estimates, which refer to higher average temperatures. However, because of the apparent contradiction in the data, we hesitate to conclude definitely that E_a declines with temperature.

Finally, k may have a dependence on particle size. As the dehydration is a surface reaction and the amount of bound water is proportional to the volume of a particle, the rate may vary inversely with particle size. Lima de Faria found a qualitative indication of this effect.

Fortunately, the particle sizes used in this experiment (a few tens of microns) are similar to those found on Mars (Pollack and Sagan, 1967; Morrison, Sagan, and Pollack, 1969), so the above results should be applicable to discussions of Mars.

5. IMPLICATIONS FOR MARS

In Paper I the reaction rates for goethite decomposition discussed above are used to reexamine the stability of this mineral on Mars. Below, supposing limonite to be moderately abundant on the Martian surface, we consider the consequences of our results for the physically bound water component.

We first relate the conditions at a typical locale on Mars to our laboratory vapor-pressure curves. Schorn, Spinrad, Moore, Smith, and Giver (1967) have detected approximately 15 μ (1.5×10^{-3} g/cm^2) of water vapor on the day side of the planet, with large seasonal fluctuations, which are discussed below. Allowing for condensation in the atmosphere and a low water-vapor abundance at the surface during the night, we derive a value of 10^{-6} atm or 7.6×10^{-4} torr for the partial pressure of water vapor at the Martian surface. An average element of area experiences a diurnally averaged temperature of 215°K (Morrison et al., 1969). Examining Figure 4, we see that the above-specified pressure and temperature fall between curves 2 and 3. According to Table 1, curve 2 corresponds to a molar sorbate volume of 1.7×10^{-1} for the physically bound water. To find the sorbate volume corresponding to the Martian conditions specified above, we suppose that sorbate volume scales linearly with pressure at a given temperature (Henry's Law), a relationship that is valid for sufficiently small sorbate volumes. Under these assumptions, a molar sorbate volume of 3.7×10^{-2} is obtained. Below, we will assume that such a figure is true at all Martian locales, although its exact value is of little consequence for these considerations. Similarly, according to Table 2, a heat of sorption of about 12.5 kcal/mole applies.

Schorn et al. (1967) have reported significant variations with position of the abundance of water vapor on Mars. Table 3 contains a summary of these observations. Each of the five observations listed represents at least several days of viewing. The symbol η represents the heliocentric longitude of Mars,

D_E the latitude of the subterrestrial point (+ indicating that it lies in the northern hemisphere), and W^* the amount of water vapor detected in microns of precipitable H_2O. Because of the tilt of the Martian axis of rotation with respect to the Earth, as indicated by the value of D_E, more than half of the observable disk lies in the northern hemisphere, and the southern midlatitudes were viewed obliquely, while the southern polar regions were not viewed at all. Accordingly, the terms northern and southern hemispheres in Table 3 are somewhat ill defined. Schorn et al. attribute their findings to the vaporization of water ice in the northern polar cap, with subsequent transport of water vapor to the cooler hemisphere by winds, and the eventual formation of a new polar cap in that hemisphere.

Table 3. Summary of the observations by Schorn et al. (1967) of the variation in the distribution of water vapor on Mars with season.

Season†	η	D_E	W^*	Distribution
Start of spring	93°	+15°	<15 μ	none observable
Early spring	115°	+20°	<15	none observable
Late spring	140°	+22°	15	only northern hemisphere
Midsummer	200°	+23°	10	similar amounts in both hemispheres
Midsummer	210°	+25°	25	more in southern hemisphere

† For the northern hemisphere.

Figure 4 suggests an alternative explanation. The equilibrium vapor pressure of limonite varies rapidly with temperature. Thus, quite apart from condensation, the colder hemisphere of Mars will have a smaller atmospheric water-vapor content as a result of physical sorption on limonite grains. Indeed, as observed above, physical sorption will tend to take place in preference to condensation, and the formation of a water polar cap will be greatly inhibited.

We now estimate the magnitude of seasonal variation in vapor pressure expected on the basis of physical sorption. We first show that variations in the water-vapor partial pressure can be treated as isosteric processes by comparing the average amounts of physically bound and atmospheric water. Calculations by Morrison et al. (1969) indicate that diurnal temperature variations propagate to a depth of about 1 cm. Since the thermal skin depth varies as the square root of the characteristic period, seasonal temperature changes will propagate to a depth of about 25 cm. We will initially consider only the layer of material that undergoes seasonal changes but has a constant temperature over a day. With the molar volume specified above and a density of material of 1 g/cc (Sagan and Pollack, 1965), there is 1×10^{-1} g/cm^2 of physically bound water in this layer compared with only 1.5×10^{-3} g/cm^2 in the atmosphere. Thus, the seasonal changes in equilibrium vapor pressure, as influenced by this layer, may be considered as occurring isosterically, i.e., at constant sorbate volume.

Before performing equilibrium pressure calculations, we explore several other aspects of the response of the subsurface layers to temperature changes. Since measurements of the radar reflectivity of Martian bright areas indicate that they are porous to a depth of at least 1 m (Sagan and Pollack, 1965; Paper I), we are justified in assuming an interaction between the atmospheric water vapor and the layer undergoing seasonal temperature changes. In addition, the characteristic time scales do not exceed a Martian year ($\sim$ 2 terrestrial years). Our laboratory samples showed response times for outgassing on the order of hours. Since the thermal conductivity of powders with values similar to those of the Martian surface depend on the ambient pressure and are almost independent of composition (Leovy, 1966), gaseous transport is probably the chief heat-transport mechanism within the Martian soil. In this case, the time scale for water vapor to diffuse through the layer undergoing seasonal changes is probably comparable to the time scale for heat transfer.

A negligibly small temperature change is implied for substantial changes in the atmospheric water-vapor content. If all the atmospheric water vapor ($\sim 1.5 \times 10^{-3}$ g/cm^2) is absorbed, approximately 1.0 cal/cm^2 will be released. Using a density of 1 g/cm^3 and a specific heat of 0.25 cal/g (Sagan and Pollack, 1965; Paper I), we find that a rise in temperature of about 0.2°K will occur in the top 25 cm.

Finally, a water-vapor pressure gradient will exist between the top 25 cm and the layers beneath, which are at constant temperature, independent of the diurnal and seasonal fluctuations in solar illumination. In order for there to be no net flux of water vapor between these layers, the equilibrium pressure of the bottommost layer should be a mean of the values implied for the upper layers. In general, this implies a somewhat larger sorbate volume for these deep layers (cf. Figure 4 and discussion below).

The variation in equilibrium vapor pressure with temperatures can be computed readily from the Clausius-Clapyeron equation, with a heat of sorption equal to 12.5 kcal/mole. As the upper 25 cm is participating in the seasonal temperature change and only the top centimeter undergoes significant diurnal temperature fluctuations (Morrison et al., 1969), we will consider only diurnally averaged temperature values. Heat-conduction calculations reported by Morrison et al. indicate that when the surface temperatures have peak values of 304° and 229°K, the average temperature equals approximately 229° and 189°K, respectively. Using these results, we have estimated the average temperatures $\bar{T}$ for several peak temperatures T_p of interest. These figures are given in Table 4. Also given are the corresponding equilibrium atmospheric water-vapor amounts W^* associated with the average temperature values. In estimating W^*, we have assumed that W^* scales as the equilibrium pressure and have normalized W^* so as to yield a value of 15 μ at 215°K, in accord with earlier discussions.

Table 4. Theoretical dependence of the Martian atmospheric water-vapor content W^* upon the diurnally averaged temperature $\overline{T}$.

T_{max} (°K)	$\overline{T}$ (°K)	W^* (in precipitable μ)†
305	230	2.0×10^2
295	224	7.1×10^1
285	219	3.0×10^1
280	216	1.8×10^1
270	211	7.5
240	195	4.7×10^{-1}
205	176	1.8×10^{-2}

† Normalized so that $W^* = 15\ \mu$ at 215°K.

It must be emphasized that the values of W^* given in Table 4 are strictly valid only if a given locale on Mars were truly isolated from other locales at different temperatures. Atmospheric winds can be expected to modify substantially the distribution of water vapor, especially after a given region has been at a high average temperature for a long period of time.

With these words of caution, we compare the results of Tables 3 and 4. To facilitate the comparison, we use the theoretical peak surface temperatures shown in Figure 8, adapted from Sagan and Pollack (1967), for various Martian seasons and latitudes. The computed temperatures are daytime average values, and in this sense they are less than the peak daytime temperature. However, the assumed albedo (0.10) is substantially lower than now-accepted values, and the resulting overestimate of the temperature results in values quite close to peak ones obtained by Morrison et al. (1969). As we wish to obtain only crude estimates of the expected variation in

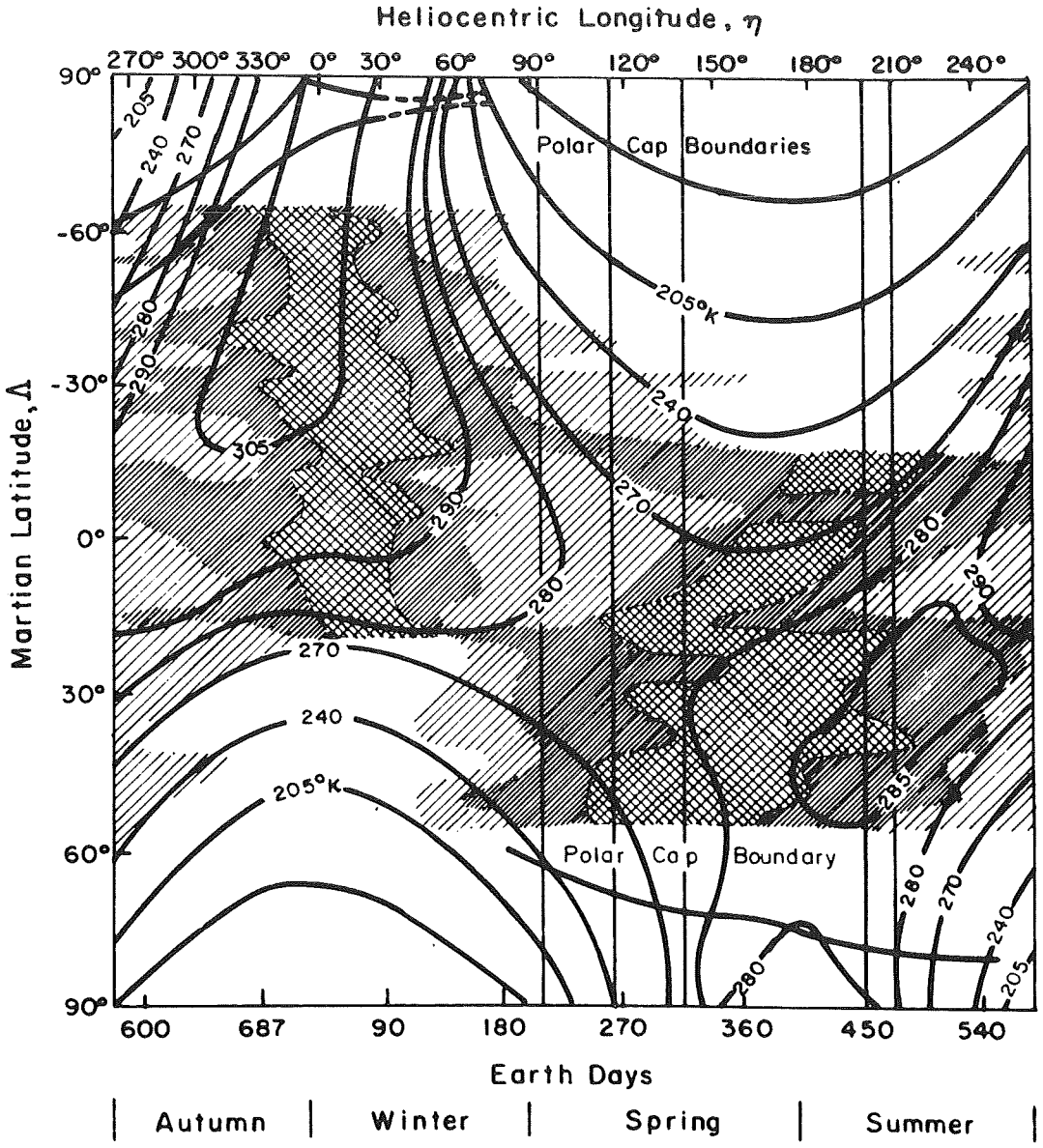

Figure 8. Calculated daytime temperatures of the Martian surface. The vertical coordinate indicates the latitude, with a negative value denoting the southern hemisphere; the horizontal coordinate is the location of Mars in its orbit about the Sun, expressed as the heliocentric longitude, or equivalently the season of the year in the northern hemisphere. The vertical lines indicate the time at which a given set of water-vapor measurements were obtained by Schorn et al. (1967). The various crosshatchings indicate the extent of seasonal darkening of dark areas. This figure was adapted from Sagan and Pollack (1967).

equilibrium pressure, Figure 6 is adequate. The vertical lines correspond to the heliocentric longitudes given in Table 3. At the time of the two sets of observations in early spring for the northern hemisphere, the peak temperatures at most locales are 270°K or lower and the values of W^* given in Table 4 are compatible with the observed upper limit of 15 μ. During the late-spring measurements, most of the northern hemisphere is at 280°K, while the southern hemisphere is at its coldest, with temperatures far below 270°K. The expected and observed topographical distributions of water vapor are again in agreement. At the highest temperatures determined by solar insolation on Mars, water-vapor partial pressures are quite high; abundances of several hundred precipitable microns should easily be detectable by flyby or orbital spectrometers. Hot spots due to geothermal activity (Lederberg and Sagan, 1962), provided they are not too old, should show even higher partial pressures. Finally, during midsummer, the location of the highest peak temperatures has shifted somewhat northward, but not so far as apparently indicated by the observations. These arguments are valid even if limonite is present only as a thin patina on particles of other composition. Only if there is less bound surface water than free atmospheric water — a very unlikely circumstance — does the argument falter. In summary, within the present observational and theoretical uncertainties, the observations by Schorn et al. (1967) of the variation in the distribution of Martian water vapor with season are compatible with the expected temperature dependence of water vapor in quasi-equilibrium with an absorbing layer of limonite. Thus, the observations of Schorn et al. do not necessarily imply large amounts of condensed water in the polar caps.

Comparing Figure 8 with Table 4, we see that significantly more water vapor should be detected in the late spring and early summer for the southern hemisphere than that found during late spring for the northern hemisphere. However, this may not be a unique prediction. Flyby and orbiter missions to Mars, because of their enhanced spatial resolution, offer the best chance of determining whether sorption or condensation processes control seasonal and topographical variations in the atmospheric water-vapor content.

In a similar fashion, we can expect that sorption processes in the layer undergoing diurnal temperature variations (approximately the upper 1 cm) will inhibit the formation of frosts directly upon the ground during the night. The surface temperature of equatorial areas on Mars varies over the day from about 180° to 300°K (Sinton and Strong, 1960; Morrison et al., 1969). Let us suppose that at sunrise the surface material had the same molar sorbate volume as the subsurface material, about 3.7×10^{-2}. Then the surface material, whose depth and density are 1 cm and 1 g/cc, respectively, would contain 3.8×10^{-3} g/cm^2 of bound water, an amount comparable to that in the atmosphere; about 2.6 cal/cm would be required to cause complete vaporization. As the sun supplies about 200 cal/cm^2 near the equator, complete vaporization could occur over the day. When the temperature rises above about 225°K, the constant temperature below a depth of 1 cm, the equilibrium pressure of the surface material will exceed the ambient partial pressure of water vapor and the surface material will begin to lose bound water to the atmosphere. During the day the lower atmosphere is convectively unstable (Gierasch and Goody, 1968), and so the released water will be distributed throughout the warmer portion of the Martian troposphere ($\sim$ 5 km in altitude). Since the presumed bound-water content is only comparable to the initial amount of atmospheric water, we see from Figure 4 that equilibrium near noon is achieved only through a movement predominantly to the right in the diagram, i.e., a very substantial reduction in sorbate volume.

During the night the reverse situation will occur. The surface layers will sorb atmospheric water vapor. However, since the portion of the atmosphere closest to the ground exhibits an inversion layer during the night (Gierasch and Goody, 1968), transport of water vapor to the ground will be quite slow. If transport is chiefly by molecular diffusion, then standard diffusion equations (Present, 1958), applied to Martian conditions, imply that the ground will receive water vapor from only the lowest 10 m of the atmosphere and so will regain only 2×10^{-3} of the amount lost during the day.

We have seen that if initially the surface layer had a sorbate volume comparable to that of the subsurface layers, it would lose most of the bound water over a period of a day. To meet the conditions of no net change in bound water over a day, the surface should gain water from the atmosphere during the cooler portion of the sunlit hours, while losing water during the warmer hours. At night the vapor pressure at the very surface will be very low, although little water is absorbed. During the day the partial pressure will be close to the value typical of most of the atmosphere. We have already implicitly made use of these conclusions in assigning a value of 10^{-6} atm as the average partial pressure at the surface, although a value about twice as large may be valid for most of the lower atmosphere. An examination of Figure 4 shows that the equilibrium pressure achieved at the surface will be somewhere between curves 3 and 4, with the molar sorbate volume about an order of magnitude less than that below and the bound-water content a similar amount less than the atmospheric content. During the day equilibrium is approached by horizontal movements in the diagram, i.e., through changes in sorbate volume, while at night the movement is chiefly vertical, i.e., the pressure is changed.

REFERENCES

AMERICAN PUBLIC HEALTH ASSOCIATION

1965. Phenanthroline method. In Standard Methods for Examination of Water and Wastewater. Amer. Pub. Health Assoc., New York, pp. 156-158.

BINDER, A. B., and CRUIKSHANK, D. P.

1963. Comparison of the infrared spectrum of Mars with the spectra of selected terrestrial rocks and minerals. Comm. Lunar Planet. Lab., Univ. Ariz., vol. 2, no. 37, pp. 193-196.

CHANDRASEKHAR, S.

1960. Radiative Transfer. Dover Publ. Inc., New York, 393 pp.

DOLLFUS, A.

1957. Étude des planètes par la polarisation de leur lumière. Ann. d'Astrophys., Suppl. No. 4, 114 pp.

DUSHMAN, S.

1962. Scientific foundations of vacuum technique. J. Wiley & Sons, Inc., New York, 806 pp.

GIERASCH, P., and GOODY, R.

1968. A study of the thermal and dynamical structure of the Martian lower atmosphere. Planet. Space Sci., vol. 16, no. 5, pp. 615-646.

GOLDSZTAUB, S.

1935. Étude de quelques dérives de l'oxide ferrique ($FeO \cdot OH$, FeO_2Na, FeOCl): détermination de leurs structures. Bull. Soc. Franc. Miner. et Crystallographie, vol. 58, pp. 6-76.

LEDERBERG, J., and SAGAN, C.

1962. Microenvironments for life on Mars. Proc. Nat. Acad. Sci., vol. 48, no. 9, pp. 1473-1475.

LEOVY, C.

1966. Note on thermal properties of Mars. Icarus, vol. 5, pp. 1-6.

LIMA DE FARIA, J.

1963. Dehydration of goethite and diaspore. Zs. f. Kristallographie, vol. 119, pp. 176-203.

MORRISON, D., SAGAN, C., and POLLACK, J. B.

1969. Martian temperatures and thermal properties. Icarus, vol. 11, pp. 36-45.

POLLACK, J. B., and SAGAN, C.

1967. An analysis of Martian photometry and polarimetry. Smithsonian Astrophys. Obs. Spec. Rep. No. 258, 97 pp.; also in Space Sci. Revs., vol. 9, no. 2, pp. 243-299, 1969.

POLLACK, J. B., WILSON, R. N., and GOLES, G. G.

1969. A reexamination of the thermodynamic stability of geothite on Mars. Journ. Geophys. Res. (in press).

POSNJAK, E., and MERWIN, H. E.

1919. The hydrated ferric oxides. Amer. Journ. Sci., ser. 4, vol. 47, pp. 311-348.

PRESENT, R. D.

1958. Kinetic Theory of Gases. McGraw-Hill, New York, 280 pp.

SAGAN, C., PHANEUF, J. P., and IHNAT, M.

1965. Total reflection spectrophotometry and thermogravimetric analysis of simulated Martian surface materials. Icarus, vol. 4, pp. 43-61.

SAGAN, C., and POLLACK, J. B.

1965. Radio evidence on the structure and composition of the Martian surface. Radio Sci., vol. 69D, p. 1629.

1967. A windblown dust model of Martian surface features and seasonal changes. Smithsonian Astrophys. Obs. Spec. Rep. No. 255, 44 pp.

SCHORN, R. A., SPINRAD, H., MOORE, R. C., SMITH, H. J., and GIVER, L. P.

1967. High-dispersion spectroscopic observations of Mars. II. The water-vapor variations. Astrophys. Journ., vol. 147, pp. 743-752.

SHARONOV, V. V.

1961. A lithological interpretation of the photometric and colorimetric studies of Mars. Soviet Astron. – AJ, vol. 5, pp. 199-202.

SINTON, W. M., and STRONG, J.

1960. Radiometric observations of Mars. Astrophys. Journ., vol. 131, pp. 459-469.

BIOGRAPHICAL NOTES

JAMES B. POLLACK received the A. B. degree from Princeton in 1960, the M. A. degree from the University of California at Berkeley in 1962, and the Ph. D. degree from Harvard University in 1965.

Dr. Pollack held appointments as physicist on the staffs of the Smithsonian Astrophysical Observatory and Harvard College Observatory from 1965 to 1968. He is currently a senior research associate with the Laboratory for Planetary Studies, Cornell University.

His research specialties include theoretical studies of planetary atmospheres, cloud layers, and surfaces.

DOUGLAS PITMAN received the B. S. degree from Dartmouth College in 1947 and the M. S. degree from the University of New Hampshire in 1949.

He has held an appointment as physical chemist on the staff of the Smithsonian Astrophysical Observatory since 1964.

His investigations include solar and stellar studies and research on low-temperature physics of ices, physical properties of solids and gases, and design of high vacuum apparatus.

BISHUN N. KHARE received the B. Sc. and M. Sc. degrees from Banaras Hindu University, India, in 1953 and 1955, respectively, and the Ph. D. degree from Syracuse University in 1961.

From 1966 to 1968 he held joint appointments as physicist on the staffs of Harvard College Observatory and the Smithsonian Astrophysical Observatory. Dr. Khare is currently a senior research physicist with the Laboratory for Planetary Studies, Cornell University.

His principal areas of research include molecular structure and spectroscopy, applications of spectroscopic techniques to the study of compounds synthesized in primitive terrestrial and contemporary planetary atmospheres by photochemical reaction, and hydrogen bonding among molecules of biological interest.

CARL SAGAN received the A. B., S. B., S. M., and Ph. D. degrees from the University of Chicago in 1954, 1955, 1956, and 1960, respectively.

From 1962 to 1968 he held joint appointments on the staffs of Harvard College Observatory and the Smithsonian Astrophysical Observatory. Dr. Sagan is currently Director, Laboratory for Planetary Studies, and Associate Professor of Astronomy, Cornell University. He is also a consultant to the National Aeronautics and Space Administration and the National Academy of Sciences.

Dr. Sagan's investigations include studies of the physics and chemistry of planetary atmospheres and surfaces, exobiology, and the origins of life.

NOTICE

This series of Special Reports was instituted under the supervision of Dr. F. L. Whipple, Director of the Astrophysical Observatory of the Smithsonian Institution, shortly after the launching of the first artificial earth satellite on October 4, 1957. Contributions come from the Staff of the Observatory.

First issued to ensure the immediate dissemination of data for satellite tracking, the reports have continued to provide a rapid distribution of catalogs of satellite observations, orbital information, and preliminary results of data analyses prior to formal publication in the appropriate journals. The Reports are also used extensively for the rapid publication of preliminary or special results in other fields of astrophysics.

The Reports are regularly distributed to all institutions participating in the U. S. space research program and to individual scientists who request them from the Publications Division, Distribution Section, Smithsonian Astrophysical Observatory, Cambridge, Massachusetts 02138.